HEAT PUMP MODELING: A PROGRESS REPORT*

R. D. Ellison
F. A. Creswick
C. K. Rice
Energy Division

W. L. Jackson
S. K. Fischer
Computer Sciences Division

Oak Ridge National Laboratory
Oak Ridge, Tennessee 37830

Abstract

Computer models of the performance of heat pumps and of individual components are described; preliminary results from system improvement studies using these models are presented.

The system model which is based on the underlying physical principles, rather than empirical data, uses a calculational scheme used previously by Hiller and Glicksman. It is generalized so that it may be used to calculate performance and efficiency over a broad range of operating conditions. Its intended use is the investigation of changes in system performance brought about by modifications of the individual components, and to aid in gaining detailed understanding of the interactions between components. Examples of predicted improvements in performance based on the use of these programs are presented.

New heat exchanger models, based on a tube-by-tube computational approach, may be used by the system model when appropriate. In these models, the thermal and fluid flow performance of each tube in the heat exchanger is computed individually using local temperatures and heat transfer coefficients. Tube circuiting sequences may be specified by the user, the joining or branching of parallel refrigerant circuits is accommodated, and appropriate mixing expressions are used. Air-side correlations for any surface geometry may be specified. Comparison of calculated and observed performance parameters for heat exchangers in our laboratory are shown.

1. Introduction

The evaluation of possible improvements to a heat pump can be performed accurately and expeditiously by mathematical analysis. If such analysis is to serve as a useful guide to the more expensive and time consuming laboratory testing of proposed improvements, it must be thorough. A change in the performance of any component of the system may affect the performance of other components, so it is necessary to analyze the whole system under a variety of operating conditions in order to determine the value of a single change of component or configuration. Obviously, a repetitious task of such magnitude should be undertaken with the aid of computers. This paper is a report of the heat pump computer models developed and used at the Oak Ridge National Laboratory. It is a progress report because continued use of the models suggests changes to the computer program; it is expected that improvements will be made as long as the program is in use. Thus far, the program has been used mostly for heating mode calculations.

In developing our model we have sought to avoid duplication of effort by building, where possible, on previous efforts. Many of the sophisticated heat pump models are not available to the general user; they are held as proprietary information by their sponsors. Two of the outstanding models available in the open literature are the Westinghouse Model,[1] prepared for EPRI under the direction of Stephen Veyo, and the MIT model, an elegant trio of programs written by Carl Hiller and Leon Glicksman.[2] The present authors adopted an approach similar to that used by Hiller and Glicksman and have made extensive use of some of their subroutines, particularly the excellent package for calculating the thermodynamic properties of refrigerants. A preliminary version[3] of the present authors' heat pump model is available from the National Technical Information Service.

The intended use of the Oak Ridge heat pump model is to explore the effect of component improvements on system capacity and efficiency. For this purpose, models based on the underlying physical principles, as opposed to those that depend on empirical data, are more useful. The physically based model generally provides more explicit detail of the operational interactions of the components, information that leads to better understanding of the operation of the system. While this kind of model is more time consuming to develop, it need not be excessively costly to use. Each of the examples of results displayed later in this paper was taken from computer runs of less than 20 sec on our IBM 360/91 computer.

2. The ORNL Heat Pump Model

The ORNL heat pump model calculates the thermal performance, the heating or cooling capacity, and the coefficient of performance (COP) of the system for a given set of operating conditions. Inputs to the program are substantially the same as those described in detail in the preliminary report of the model.[3] They include the dimensions of the tubing and fins in the heat exchangers, dimensions of the interconnecting pipes, the inlet air temperatures and flow rates at the heat exchangers, the desired subcooling at the condenser exit, and the evaporator exit superheat. Initial estimates of the refrigerant saturation temperature in each heat exchanger are supplied to the program. The parameters required for the compressor and its motor include the displacement and clearance volume ratio, along with efficiency and loss parameters determined from initial calibration runs of the compressor model as described later in this report.

Outputs from the model include the capacity and COP mentioned above along with refrigerant pressure changes across each component, the air pressure drops across the heat exchangers, the overall heat exchanger effectiveness, the refrigerant thermodynamic states at appropriate points in the circuit, the air temperature at exit from the heat exchangers, and the power consumption by the two air fan motors and the compressor motor.

Detailed lists of the input data, samples of the output, and a listing of the FORTRAN IV source program will be available in future reports.

2.1 Organization of the Model

The model is organized in three principal sections, the first of which includes the compressor model. It establishes the refrigerant mass flow rate (based on the initial estimates of the refrigerant saturation conditions at the heat exchangers), thermodynamic states at appropriate points in the refrigerant circuit, and the compressor motor power consumption. The second and third sections are detailed models of the condenser and evaporator; they are used to predict performance by calculating energy balances at these heat exchangers. The thermodynamic cycle being modeled is shown in Fig. 1, a somewhat distorted pressure vs enthalpy (p-h) diagram. The flow diagram shown in Fig. 2 displays the sequence of calculations and the decision points.

Calculation of the refrigerant mass-flow rate and the initial estimates of the pressure drops begins by calling the compressor subroutine, as shown in the flow diagram. The state of the refrigerant at point 1a on the p-h diagram is established from the estimated evaporating saturation temperature, the specified superheat of the vapor (quality is used if evaporation is incomplete), and the suction line pressure drop. Using the parameters and efficiencies specified for the compressor being modeled, and the estimated condensing temperature, the compressor routine calculates the refrigerant mass-flow rate, the compressor-motor power consumption, and the state of the refrigerant at point 2a, the compressor can exit. Finally, the compressor routine, taking account of the calculated pressure drop in the discharge line, establishes the state of the refrigerant at the entry to the condenser, point 3 on the p-h diagram.

ORNL-DWG 77-19442

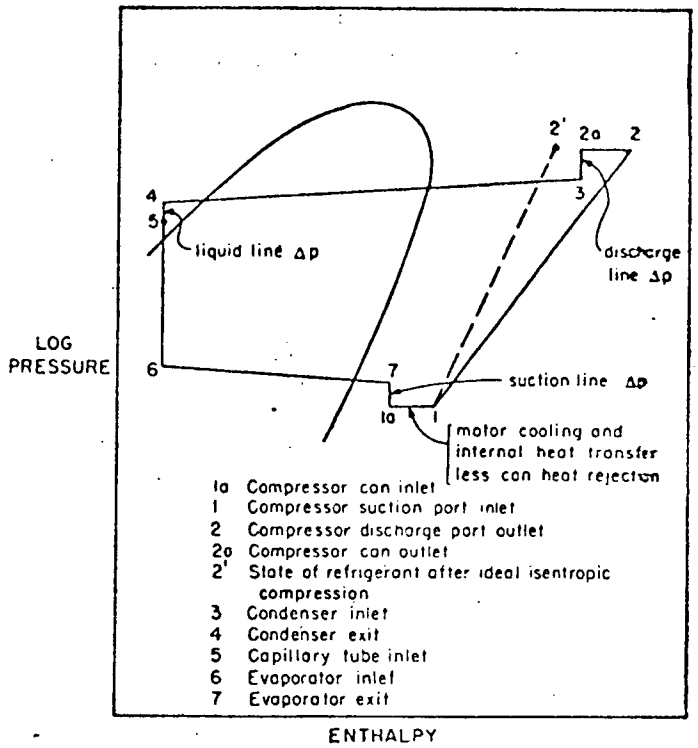

Fig. 1 Pressure vs enthalpy diagram for the heat pump cycle.

In order to obtain an estimate of the thermodynamic state of the refrigerant at the condenser exit, the pressure drop through the condenser is calculated as though the entire condenser were experiencing two-phase flow for the first iteration; thereafter the more exact pressure drop from the condenser routine is used. Thus, the pressure at point 4 of the p-h diagram is found. Calculation of the pressure drop in the liquid line, from condenser to the flow metering device, yields the refrigerant pressure at entry to that device, point 5. At this point in the calculation sequence, estimates of the heat transfer rates in the two heat exchangers may be made, using the refrigerant mass-flow rate and the estimated enthalpy change across each heat exchanger. These estimates, when compared to the more exact calculation of the heat transfer rates in the heat exchanger routines, are useful in checking the convergence of the loops over those sections of the program.

The mass-flow rate and refrigerant states calculated for the condenser entry are used, along with the air-flow rate, inlet air temperature and the geometric description of the condenser, as input to the condenser model. This subroutine calculates an energy balance between refrigerant and air to find the heat rejection rate of this heat exchanger and to predict the subcooling (or quality, if condensation is incomplete) of the refrigerant leaving the condenser. This calculated subcooling is compared with the desired subcooling specified in the input to the program; iteration over the degree of subcooling is performed, while adjusting the

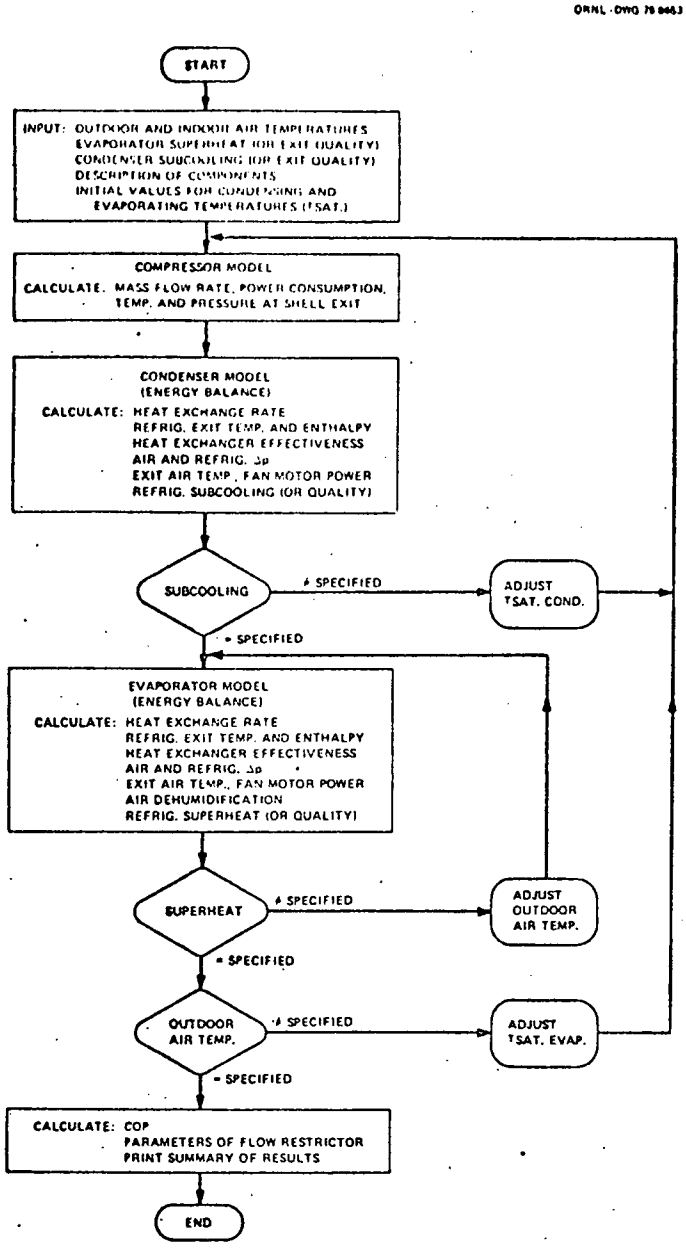

Fig. 2 Flow Diagram for heat pump computer program.

saturation temperature in the condenser, until agreement is reached. The evaporator model is then used to calculate its heat absorption rate and the superheat (or quality, if evaporation is incomplete) of the refrigerant at evaporator exit. The state of the refrigerant at the evaporator exit (superheat or quality) is compared with the desired state that is input to the program; iteration over the evaporator energy balance proceeds, while adjusting the value of the entering air temperature, until agreement is reached. Finally, the air temperature entering the evaporator, calculated above, is compared to the desired value, an input to the program; if the two are not approximately equal, the evaporating saturation temperature is adjusted, and the program iterates over the entire thermodynamic cycle until the desired evaporator air temperature is achieved.

Thus, the condensing and evaporating temperatures have been adjusted to find the operating conditions that will satisfy the air temperatures specified at the desired values of subcooling at the condenser and superheat at the evaporator exit. What remains is to calculate the COP and the characteristics of the flow control device that will produce the specified subcooling and superheat at the calculated refrigerant mass-flow rate.

The desired values of condenser subcooling and evaporator superheat must be chosen with care. If the unit being modeled uses a thermostatic expansion valve for refrigerant metering, the value of the superheat at evaporator exit is known, since the valve can be used to control this quantity. A unit that uses capillary tubes or a fixed orifice for refrigerant metering and also has a suction line accumulator may be modeled correctly using this computer program so long as the accumulator has liquid refrigerant in it; presence of the liquid in the accumulator will hold the superheat to a very low value. However, the model is not generally appropriate for a heat pump that uses capillary tubes or a fixed orifice for metering if it lacks a suction line accumulator. Such a charge-sensitive unit is expected to experience a wide range of superheat in the evaporator; it would be difficult for the user to specify a value appropriate to the selected air temperatures. For the intended use of our model, the investigation of advanced heat pumps, the present inability to handle the charge-sensitive case is not considered a serious deficiency.

In the usual application of the model, it is expected that a value will be chosen for the desired superheat, subject to the constraints discussed above, and that several computer runs will be made, each using a different value of subcooling, in order to establish an optimum value for the subcooling parameter which is consistent with the superheat chosen.

In the above calculations, the thermodynamic properties of the refrigerant are calculated using subroutines due to Kartsounes and Erth[4] as modified by Hiller and Glicksman.[2] Viscosity, thermal conductivity, and specific heat are obtained from equations that are derived from plots[5,6] of these properties (as functions of temperature) by curve fitting methods. These routines, as well as the pressure drop routines, are due to Hiller and Glicksman.[2] Single-phase pressure drops in the connecting pipes are calculated from the standard incompressible flow relation and the Moody friction factor; single- and two-phase pressure drops in the heat exchangers are calculated by the Lockhart-Martinelli[7] method.

2.2 Component Models

The overview of the system model given above, has, for the sake of clarity, glossed over the details of the component models; the important features of these models are presented in the following paragraphs.

2.2.1 Compressor model. The compressor model is based on performance and efficiency parameters that may be derived from experimental data gathered from an operating compressor in a heat pump. This approach is in contrast to the use of design parameters, and affords much simplification while retaining sufficient detail of the underlying physical

principles to make the results more meaningful than would be obtained from the use of compressor performance curves derived from calorimetric measurements. Thus, the model is compatible with its intended use in that it can predict how changes in compressor efficiency affect the heat pump system, though it cannot be used to determine what specific changes in compressor design might lead to the improved efficiency.

Six parameters are used to model the compressor: motor peak efficiency, compressor displacement, compressor volumetric efficiency, isentropic efficiency, heat rejection from the compressor can, and heat transfer from the discharge gas back to the suction gas inside the can. Four operating variables are required as input to the compressor model: can inlet pressure and temperature, can outlet pressure, and motor speed. It should be noted that the refrigerant conditions at the suction and discharge ports of the compressor, which is mounted inside the can, will generally differ from those at the can inlet and outlet. The model allows "wet" refrigerant at the can inlet, but prints a warning message if the refrigerant reaching the compressor suction port is wet.

Five energy balances are used in the model: one each for the can, suction gas, compressor, compressor motor, and discharge gas. Fig. 3 illustrates the energy balance components used.

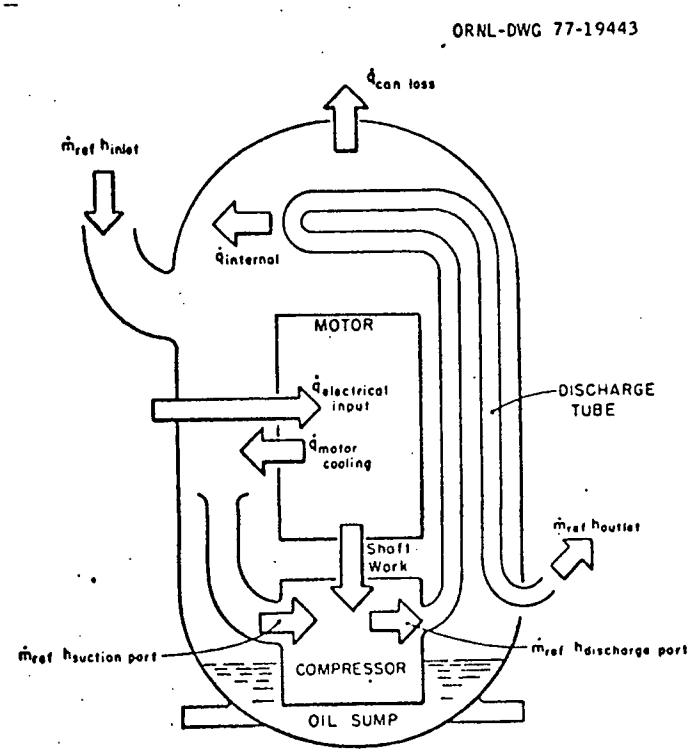

Fig. 3. Compressor can energy balance components.

For the compressor can, the enthalpy gain of the refrigerant is equal to the electrical power input minus the heat rejection from the can, so that:

$$\dot{m}_{ref}(h_{can\ outlet} - h_{can\ inlet}) - \dot{q}_{electric\ input} + \dot{q}_{can\ loss} = 0 ,$$

where $\dot{m}_{ref}$ is the refrigerant mass flow rate, h is the specific enthalpy, and $\dot{q}$ is the energy flow rate. For the suction gas, it is necessary to account for heating of the gas due to motor losses, the internal transfer of heat from the discharge, and the heat rejection from the can, with which the suction gas is in contact. Thus:

$$\dot{m}_{ref}(h_{suct\ port} - h_{can\ inlet}) - \dot{q}_{internal} - \dot{q}_{motor\ cooling} + \dot{q}_{can\ loss} = 0 .$$

For the discharge gas:

$$\dot{m}_{ref}(h_{disch\ port} - h_{can\ outlet}) - \dot{q}_{internal} = 0 ,$$

and the actual compression work is computed as:

$$\Delta h_{compressor} = h_{disch\ port} - h_{suct\ port} = \frac{\Delta h_{isentropic}}{\eta_{isentropic}} ,$$

where $\Delta h_{isentropic}$ is obtained from the thermodynamic properties of the refrigerant, and $\eta_{isentropic}$ is the input isentropic efficiency. The mass flow rate is calculated from the volumetric efficiency, η_{vol} (which is obtained from the compressor clearance volume ratio and the ratio of specific volumes at suction and discharge pressures) as:

$$\dot{m}_{ref} = \eta_{vol}(\rho DN) ,$$

where ρ is the refrigerant density at suction port, D is the compressor displacement, and N the motor speed. Routines included in the program calculate motor speed and efficiency (used in the next equation) as functions of motor load, rated power, and peak efficiency.

If all mechanical losses are dissipated by heating the refrigerant, the shaft power is proportional to the product of $\dot{m}_{ref}$ and $\Delta h_{compressor}$, so that:

$$\text{motor power input} = \frac{\text{shaft power}}{\eta_{motor}} = \frac{\dot{m}_{ref}\Delta h_{compressor}}{\eta_{motor}\ \eta_{comp}} ,$$

where η_{motor} is the motor efficiency and η_{comp} is the compressor mechanical efficiency. The heat rejected by the motor to suction gas is:

$$\dot{q}_{motor\ cooling} = (1 - \eta_{motor})(\text{motor power input}) .$$

Since the suction-gas heating is a function of motor power input, and the motor power input is in turn a function of the state of the suction gas entering the compressor suction port, an iterative computational procedure is required.

The compressor model described above must be calibrated before it can be used. This calibration was accomplished from estimates of can heat loss determined analytically and experimentally; internal heat losses estimated analytically; and typical values of clearance volume ratios, and isentropic and motor efficiencies. Parametric studies using the compressor model determined that such estimates were sufficient to allow the model to produce compressor performance parameters in good agreement with those observed experimentally.

2.3 Heat Exchanger Models

Two sets of heat exchanger models are available to the heat pump system model. Very detailed models that compute separately the performance of each tube in the heat exchanger will be described in a later section of this paper. The heat exchanger models used for exploratory studies, adapted from Hiller and Glicksman,[2] are faster, but less flexible in their applications. They are predicated on the conventional crossflow configuration and staggered-tube and sheet-fin construction. Principal input parameters are geometric constants which include the tube diameter, length, and spacing; fin pitch and thickness; number of parallel refrigerant circuits; and overall dimensions. All necessary correlations for fluid thermal properties, heat transfer coefficients, and flow friction factors, for both air and refrigerant side, are internal to the computer program.

The models for both condensing and evaporating are based on the methods of Kays and London,[8] using the effectiveness vs. number of transfer units (N_{tu}) equations for a crossflow heat exchanger with both fluids unmixed, or rather approximations to those exact equations, developed by Hiller and Glicksman,[2] that may be cast in closed form. Use of the equations for both fluids unmixed imposes some restrictions on the rigorous application of the models to heat exchangers that employ complex refrigerant circuiting, but is sufficient for use of the models in exploratory studies.

Heat transfer correlations for single-phase refrigerant flow inside tubes and air-side flow are based on Kays and London[8] data in the form of "j" factor ($N_{St} \cdot N_{Pr}^{2/3}$) as a function of Reynolds number. Condensing coefficient correlations are from Traviss, Baron, and Rohsenow,[9] and those for evaporation from Tong.[10] Two-phase pressure drops are computed using the Lockhart-Martinelli correlation,[7] while single-phase pressure drops are calculated by conventional pipe flow methods.

2.3.1 Condenser. At the outset of the condenser program, a computation is made to determine whether the tube wall temperature at the condenser entrance is less than the refrigerant saturation temperature. If it is not, the fraction of the condenser coil required for desuperheating the refrigerant is computed, and average air- and refrigerant-side heat transfer coefficients for the region are calculated. Otherwise it is assumed that two-phase flow begins at the entrance, even though the bulk refrigerant temperature may be above saturation. The fraction of the coil required to complete condensation, that is, the length of coil in two-phase flow, is computed, and the average heat transfer coefficients for this region are found. The remaining fraction of the coil is, of course, in single-phase liquid flow; the amount of subcooling in this region is calculated. In the event that the sum of the fractions of the coil required for desuperheating and for two-phase flow is greater than unity, condensation is incomplete. In this case, the exit quality must be calculated and the average heat transfer coefficients for the two-phase region modified.

Finally, the heat transfer rate of the condenser is calculated as the sum of those rates from the three flow regions in the heat exchanger, and the average temperature of the outlet air is taken as the weighted average of the temperature of the air exiting each region. From the total air pressure drop across the coil, the power consumption of the fan motor is estimated.

2.3.2 Evaporator. The model for the evaporator is similar to that for the condenser with the additional provision for computing the amount of air dehumidification, if any. In the method used, it is assumed that the heat transfer coefficient is unaffected by the presence of condensed moisture, and a heat-transfer/mass-transfer analogy is used to compute the rate of moisture removal. Total heat transfer rate is determined on the basis of enthalpy difference.

Initally, a computation is made to determine the dew point of the entering air and whether the wall temperature at the entrance is less than the dew point of the air. If it is determined that moisture condensation from the air will not occur at the entrance, the fraction of the coil used only for sensible heat transfer is computed. Since the air is being cooled in the evaporator while the temperature of the refrigerant is essentially constant in the two-phase region, the wall temperature will decrease in the direction of airflow and may drop below the dew point. The performance of that section of the evaporator having two-phase evaporation on the refrigerant side and dehumidification on the air side is then computed. Finally, the amount of refrigerant superheating in the remaining fraction of the coil is computed with no allowance for further dehumidification on the air side. Incomplete evaporation is treated in similar fashion to incomplete condensation in the condenser model.

2.4 Results from the Heat Pump System Model

Table 1 shows the results from validation runs of the heat pump model. The computer program was executed using the operating conditions for two of

Table 1. Comparison of calculated and observed performance of an air-to-air heat pump

	Run 10		Run 2	
	Observed	Calculated	Observed	Calculated
Compressor Model				
Refrigerant mass-flow rate (lbm/hr)	329	328	353	361
Compressor motor power input (kW)	4.09	4.00	4.17	4.19
Refrigerant temperature at compressor exit (°F)	224	220	229	226
Saturation temperature at compressor inlet (°F)	24.6	23.0	28.3	28.5
Refrigerant temperature at compressor inlet (°F)	42.8	41.7	53.7	53.9
Saturation temperature at condenser entry (°F)	124.3	123.9	130	129
Refrigerant pressure at capillary tube entry (psia)	275	274	295	290
Condenser Model				
Air temperature, entry (°F)	72.5	72.5	69.6	69.6
Air temperature, exit (°F)	101.2	98.1	101.5	98.2
Refrigerant temperature, entry (°F)	201.7	197.8	205.5	202.4
Refrigerant temperature, exit (°F)	79.8	79.4	77.7	76.7
Refrigerant subcooling (F°)	44.1	44.1	52.2	52.2
Heat rejection rate (Btu/hr)	32,064	31,691	34,594	35,302
Fan-motor power consumption (kW)	0.608	—	0.590	—
Evaporator Model				
Air temperature, entry (°F)	41.7	41.7	51.0	51.0
Air temperature, exit (°F)	33.5	35.0	41.5	42.4
Refrigerant temperature, exit (°F)	38.7	37.1	49.5	49.5
Saturation temperature, exit (°F)	—	27.1	—	32.7
Refrigerant superheat (F°)	—	10.1	—	16.8
Heat absorption rate (Btu/hr)	25,659	25,084	28,091	28,530
Fan-motor power consumption (kW)	0.511	—	0.499	—
System Performance				
Coefficient of performance	1.92	1.93	2.04	2.07

the heating mode runs of a heat pump in our laboratory as input data, along with geometric descriptions of the unit and the compressor calibration parameters discussed earlier. Calculated values of refrigerant mass-flow rate, compressor power consumption, heat exchange rates, refrigerant and air temperatures and COP are compared to those observed in laboratory experiments reported to this conference last year by Domingorena.[11] Inspection of the table reveals that agreement is good. The calculated mass-flow rates, power consumption, heat exchange rates, and COP fall within 2.3% of the observed values. The largest difference between calculated and observed temperatures, 4 F°, is for the refrigerant temperatures at the compressor exit.

It would be pleasant to report that we simply entered the data, ran the computer program, and such nice results appeared without further effort. But, as almost always happens, the validation runs revealed weaknesses in the model. The calculated refrigerant pressure drops in the suction line were smaller than observed, as were the values calculated for the fan-motor power consumption. The results shown in Table 1 were obtained using the observed values for these quantities, admittedly a stop gap measure pending the development of better models of the reversing valve and the fan power consumption. In validating the model, emphasis has been placed, so far, on heating mode calculations.

Table 2 shows some preliminary predictive results obtained from the use of the heat pump program. The examples selected are intermediate results from a parametric study of the increased heat pump efficiency that may be obtained while using conventional components; they show the combined effects due to the changes in the component parameters listed in Table 3. The operating conditions are those for indoor and outdoor air temperatures of 70 and 47°F, respectively, with the outdoor relative humidity at 70%. The "base" case parameters are those for one of the heat pumps in our laboratory; those for the "improved" cases do not necessarily represent optimum or economically justified choices, but rather steps in that direction.

Table 2. Predicted performance improvement

Performance Parameter	Base Case	Case A	Case B
Coefficient of performance	2.29	3.47	3.97
Heating capacity (Btu/hr)[a]	40,404	37,993	39,409
Condenser effectiveness (%)	71.8	82.6	86.04
Condensing temperature (°F)	130.5	125.1	119.4
Evaporator effectiveness (%)	67.1	83.5	84.81
Evaporator temperature (°F)	28.8	28.4	27.9
Condenser fan power (Btu/hr)	1,291	346	455
Evaporator fan power (Btu/hr)	1,327	335	331
Compressor motor power (Btu/hr)	15,056	10,280	9,130

[a]Includes heat from indoor fan motor

Case A is based on an arbitrary increase of about 50% in the face area of both heat exchangers, and the use of the best available compressor and compressor motor. Case B has heat exchangers with twice the face area of the base case, but still within the range of areas used in currently available high efficiency heat pumps; the mechanical efficiency of the compressor and the motor efficiency have, however, been pushed to an extreme. In both improved cases, the volumetric air flow rates have been reduced from the base case in order to reduce fan power consumption while maintaining reasonable air to refrigerant approach temperatures.

Table 3. Component parameters for improved performance

Parameter varied	Base Case	Case A	Case B
Condenser face area (ft^2)	3.17	4.75	6.33
Evaporator face area (ft^2)	5.19	8.73	10.39
Condenser airflow rate (cfm)	1,200	800	900
Evaporator airflow rate (cfm)	2,162	1,800	2,000
Isentropic compression efficiency (%)	70	75	80
Compressor volume ratio	0.10	0.10	0.08
Compressor motor efficiency (%)	65	88	92
Compressor shell heat loss (Btu/hr)	4,500	1,000	800
Condenser subcooling (F°)	50	30	30

The significant increases in COP are seen to have been achieved while holding the heating capacity almost constant. These preliminary results have not been optimized with regard to performance or cost effectiveness. Such optimization will be the subject of later reports, as will the compromises required in order to maintain good performance in both heating and cooling modes of operation.

3. Advanced Heat Exchanger Models

While the heat exchanger models described above will continue to be useful the authors judge that the form of those models will limit their applicability for certain types of investigation. With those models, the conventional tube-and-sheet-fin heat exchanger construction is the only geometry that can be accomodated; only a pure crossflow arrangement (with both fluids unmixed) and equivalent parallel, unbranched refrigerant flow circuits can be modeled rigorously.

In practice, other types of heat exchanger geometries are in current use, such as spine-fin and bristle-fin tubes. There is considerable art involved in devising refrigerant circuiting through the heat exchangers in order to obtain maximum thermal effectiveness. Such circuiting usually departs from the pure crossflow arrangement; one fluid is usually mixed. Accordingly the decision was made to develop more general heat exchanger models, and eventually to incorporate them into the heat pump system model.

The new heat exchanger models are based on a tube-by-tube computational approach. The thermal and fluid-flow performance of each tube (the length of tube between two return bends in the conventional geometry) is computed individually, based on local temperatures and heat transfer coefficients. A specified tube circuiting sequence is followed, the joining or branching of parallel refrigerant circuits is accommodated, and appropriate mixing expressions are used. Provision is made for entering, as input data, the air-side correlations for any given surface geometry.

3.1 Individual Tube Heat Transfer and Pressure Drop Calculations

For condensing, equations by Traviss, Baron, and Rohsenow[9] for heat transfer, and the methods of Lockhart and Martinelli[7] for pressure drop were used. The evaporator model incorporates the methodology and correlations of Chaddock and Noerager,[12] Dickson and Gouse,[13] and of Pierre.[14] The computational routines formulated for modeling the thermal performance and pressure losses of individual tubes are:

- refrigerant condensing heat transfer coefficient and pressure drop;
- refrigerant evaporating heat transfer coefficient and pressure drop;
- air-side heat transfer coefficient and pressure drop;
- effectiveness and heat flux for a condenser tube;
- effectiveness and heat flux for an evaporator tube.

The routines are operational and have been tested, but not yet subjected to extensive use; efforts will continue to refine the correlations, particularly those for the dry-out region of the evaporator. Their success in predicting experimental results, reported below, warrants their inclusion in this progress report.

3.2 Assembly of Tubes Into a Heat Exchanger

The impetus for improved heat exchanger models is to obtain more accurate air-side calculations, to allow for greater variation of the surface geometry, and to model more rigorously the effects of complex refrigerant flow circuiting. In general, it may be expected that changes in the thermodynamic properties of the refrigerant will be much greater than those for the air as both fluids move through the heat exchanger. Accordingly, the assembly of tubes into a heat exchanger is treated as viewed from the refrigerant side in that individual tubes will be modeled in the sequence in which the refrigerant, not the air, reaches each tube. A consequence of

this choice, since the two fluids are in crossflow, is that the temperature of the air at a particular tube may not be known accurately when it comes time to model the refrigerant-side heat exchange for that tube. It is, then, necessary to calculate the performance of the heat exchanger within an iterative loop over the entire assembly of tubes.

In order to calculate the performance of tubes in the sequence in which refrigerant reaches them, a table of tube connections is used to trace the path of refrigerant flow. Usual construction methods for compact heat exchangers require that a tube receive refrigerant from no more than two tubes upstream, and in turn deliver it to no more than two tubes downstream. It is, then, sufficient to specify at most four tubes in the heat exchanger that may connect to a tube in question. It is convenient to consider the assembly as consisting of layers of tubes, with each layer being perpendicular to the direction of airflow. A tube may then be referenced by its position in a layer, and the layer number.

The first task in modeling the assemblage is to find the total resistance to flow of refrigerant through each possibly multibranched path through the heat exchanger so that the refrigerant reaching the inlet header may be apportioned among the several tubes that are connected directly to it. We may then model the entire heat exchanger by modeling first a tube that is so connected and, using the table of tube connections, selecting subsequent tubes to model in the order that refrigerant reaches them. Thus, the refrigerant properties at the outlet of one tube may serve as the inlet properties of the next, or a contributor to them if branching is involved. After all tubes in one circuit have been modeled, the process is repeated, starting with another tube that is connected directly to the inlet header. After all the tubes in the heat exchanger have been modeled, a check for convergence of the iterative process over the heat exchanger is made; when convergence has been reached, capacity of the heat exchanger is found by summing the capacities of individual tubes; averaged properties of the outlet air and refrigerant are calculated.

Details of this scheme, including the complications introduced by confluences and downstream branching, will be given in a later report along with a complete description of the routines used to calculate individual tube performance.

3.3 Results

The performance of one of the heat exchangers in our laboratory has been calculated using the tube-by-tube condenser model. The results of this calculation, which took about 6 sec on our IBM 360/91 computer, are compared to those observed in the laboratory in Fig. 4. The condenser being modeled is a tube-and-sheet-fin heat exchanger in crossflow. There are 72 tubes arranged in 3 layers of 24 tubes each, and three parallel refrigerant circuits. Refrigerant entering the front layer of tubes (the side where air enters the heat exchanger) is switched to the rear layer at tube 13, and that from the rear layer is brought to the front; one refrigerant circuit lies entirely within the middle row of tubes.

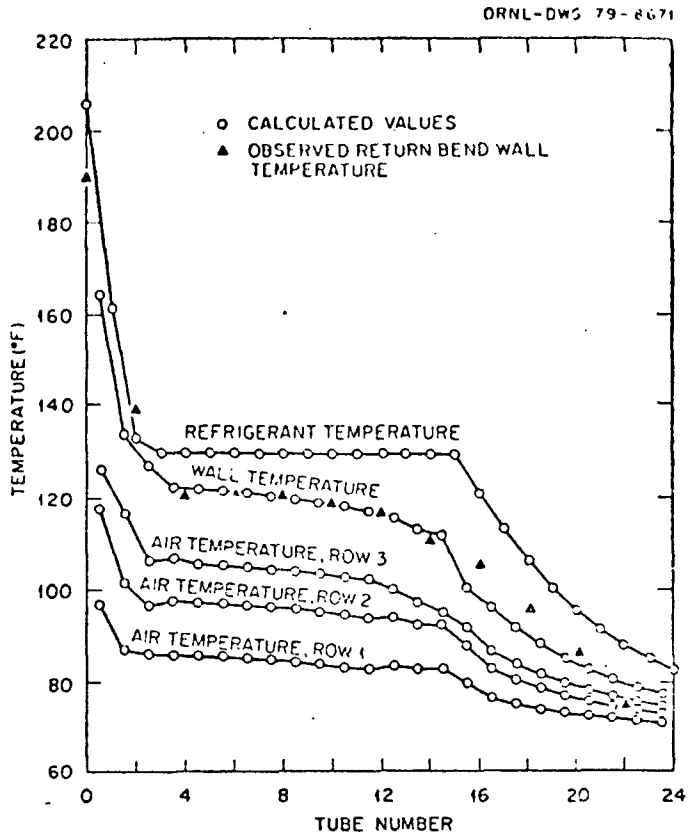

Fig. 4. Results from tube-by-tube calculation of the performance of a tube-and-sheet-fin condenser.

The top curve in Fig. 4 represents the refrigerant temperature at the exit of each tube in the middle row. The next curve down is the predicted tube wall temperature at the midpoint of each tube in the same circuit and is compared to the wall temperatures measured at the return bends. The regions containing superheated, two-phase, and subcooled refrigerant are closely predicted. The calculated wall temperatures are seen to be in good agreement with the observed values, with the greatest error near the lower temperature end of the subcooled region. The bottom three curves show the calculated air temperatures after passing over each tube. The calculated heat exchanger capacity is 34,531 Btu/hr; observed capacity is 34,950 Btu/hr.

4. Planned Modifications

The heat pump model described in this progress report is, in its present state, capable of performing most all of the tasks required for its intended use. The model can be used to predict the system performance resulting from many of the possible heat pump system improvements that are presently contemplated. It is planned, however, that additional development work will be conducted to improve the model's versatility. Some of the changes being considered are described in the following paragraphs.

The model may, in its present form, be applied to heat pump systems that use a thermostatic expansion valve or (if the system contains a suction line accumulator) a capillary tube for refrigerant metering. Some systems use a fixed orifice in critical flow for metering. We plan to add an orifice model to the program that is capable of simulating two-phase flow as well as the simpler single-phase case.

As noted in the discussion of the model validation, it was necessary to impose a larger suction line pressure drop than our model predicts. More careful consideration of the pressure drops in the minor components, such as mufflers and the reversing valve, seems to be indicated.

In its present state of development, the heat pump system model cannot be used to calculate the performance of a charge-sensitive heat pump, as was noted earlier in discussion of the specification of evaporator superheat values to be used as input data. An implicit assumption has been made that the system is charged with exactly the correct amount of refrigerant for the operating conditions. This is a satisfactory model for heat pump systems having a suction line accumulator; i.e., the accumulator is modeled satisfactorily (except for its small pressure drop) by ignoring it. However, in systems that do not employ an accumulator, there can be an excess charge under certain operating conditions. Such a system, properly charged for the cooling cycle, may contain an excess charge during heating operation as a result of the lower system pressures. The excess refrigerant will migrate to the condenser where it can partially block some of the heat transfer surface. To model correctly this type of system, a refrigerant mass inventory is necessary as well as routines for deciding where the excess refrigerant will accumulate and what the effect on the thermodynamic cycle will be. A study of possible approaches to such a model is planned.

References

1. H. S. Kirschbaum and S. E. Veyo, *An Investigation of Methods to Improve Heat Pump Performance and Reliability in a Northern Climate*, EPRI EM-319 (Research Project 544-1) January 1977.

2. C. C. Hiller and L. R. Glicksman, *Improving Heat Pump Performance via Compressor Capacity Control — Analysis and Test*, Report No. 24525-96, Heat Transfer Laboratory, Massachusetts Institute of Technology, Cambridge, Massachusetts, 1976.

3. R. D. Ellison and F. A. Creswick, *A Computer Simulation of Steady State Performance of Air-to-Air Heat Pumps*, ORNL/CON-16 (March 1978).

4. G. T. Kartsounes and R. A. Erth, "Computer Calculation of the Thermodynamic Properties of Refrigerants 12, 22, and 502" *ASHRAE Transactions*, Vol. 77, Part II, 1971.

5. American Society of Heating, Refrigeration, and Air Conditioning Engineers, Inc., *ASHRAE Handbook of Fundamentals*, New York, 1972.

6. American Society of Heating, Refrigeration, and Air Conditioning Engineers, Inc., *Thermophysical Properties of Refrigerants*, New York, 1973.

7. R. W. Lockhart and R. C. Martinelli, "Proposed Correlation of Data for Isothermal Two-Phase, Two-Component Flow in Pipes", *Chemical Engineering Progress*, 45(1):39 (1949).

8. W. M. Kays and A. L. London, *Compact Heat Exchangers*, The National Press, Palo Alto, California, 1955.

9. D. P. Traviss, A. G. Baron, and W. M. Rohsenow, *Forced Convection Condensation Inside Tubes*, Report No. 72591-74, Heat Transfer Laboratory, Massachusetts Institute of Technology, Cambridge, Massachusetts.

10. L. S. Tong, *Boiling Heat Transfer and Two-Phase Flow*, Wiley, New York, 1965.

11. A. A. Domingorena, *Performance Evaluation of a Low-First-Cost, Three-Ton, Air-to-Air Heat Pump in the Heating Mode*, Presented at the 3rd Annual Heat Pump Conference, Stillwater, Oklahoma, April 10—11, 1978.

12. J. B. Chaddock and J. A. Noerager, "Evaporation of Refrigerant 12 in a Horizontal Tube with Constant Wall Heat Flux", *ASHRAE Trans* (1966).

13. A. J. Dickson and S. W. Gouse, Jr., "Heat Transfer and Fluid Flow Inside a Horizontal Tube Evaporator, Phase III", *ASHRAE Trans* (1967).

14. B. Pierre, "Flow Resistance with Boiling Refrigerants", *ASHRAE J*, Part I: 58-65, September 1964; Part II: 73-77, October 1964.